Modeling a Low Vision Observer: Application in Comparison of Image Enhancement Methods

Cédric Walbrecq, Dominique Lafon-Pham, Isabelle Marc

Modeling a low vision observer: application in comparison of image enhancement methods

Cédric Walbrecq, Dominique Lafon-Pham, Isabelle Marc

EuroMov Digital Health in Motion, Univ Montpellier, IMT Mines Ales, Ales, France
cedric.walbrecq@mines-ales.fr

Abstract. Numerous image processing methods have been proposed to help low vision people, often relied on contrast enhancement algorithms. Their assessment is usually performed by tests on low vision subjects, which are expensive and time consuming**.** This paper presents a low vision observer model, fully customizable to fit various impaired visual performances, which may be used for early algorithm assessment, and avoiding unnecessary human tests. This model is fitted to visual performances of a subject with degenerative retinal disease, and applied to images processed by two edge enhancement algorithms, allowing to explain their performances in terms of blur reduction and color saturation improvement

Keywords: computational model; low vision; contrast sensitivity function; contrast enhancement.

1 Introduction

Over the past decade, numerous studies have been devoted to the development of assistive products for visually impaired people. Common principles of these aids are the use of one or more cameras to capture the real world environment, image processing aiming to enhance visibility, and display on virtual reality or augmented reality devices. Numerous image processing methods have been proposed, often aiming to contrast enhancement and some of them significantly improve performances for tasks as reading, facial expressions recognition or visual search [1]. These methods are often evaluated through tests on low vision subjects, with as far as possible standardized viewing conditions, assessment procedures and data analysis methods. When experimental conditions are correctly designed, and subject cohort well chosen, all these tests may give access to the "truth" about utility and efficiency of these enhancement methods. But tests on human subjects are expensive and time consuming. Moreover, due to the limited size of the test cohorts and to restrictive experimental protocols, their results may not be easily extrapolated to various degrees of visual deficiencies or different viewing conditions. Looking for faster alternatives, image researchers may turn to resort to so called "objective methods", with metrics based on mathematical parameters. This paper presents a low vision observer computational model, fully customizable to fit various impaired visual performances and different technical characteristics of displays and

lighting conditions. It is intended to be used in objective comparison of image enhancement algorithms or in assessment of any new digital interface for visually impaired people. This paper is structured as follows: brief presentation of recent works on Human Visual System (HVS) simulation and modeling is found in Section 2. The proposed model is described in Section 3. Application of this model to comparison to two contrast enhancement algorithms is discussed in Section 4. Criteria for this comparison are based on blur measurement and on color saturation assessment.

2 Related Work

Taking into account the performances and limitations of the HVS is known to improve processing in various image and video domains such as acquisition, compression, watermarking, communication, enhancement, classification, reproduction, etc. Vision is known to involve both bottom-up cues, such as luminance patterns, and top-down factors such as scene understanding. In the following, we only consider the bottom up aspect, and computational models dealing with some of the mechanisms that have significant influence on visual perception, such as light absorption, diffusion and diffraction due to the eye's optics, luminance adaptation, color representation, contrast sensitivity, frequency and orientation selective perceptual channels or visual masking. Visual saliency modeling is out of the scope of this paper. Simulation of impaired vision is achieved by modifications of appropriate parameters at these different visual information processing stages in the standard vision model. As it is known that the HVS response depends much less on the absolute luminance than on its relative local variations to the surrounding background, the Contrast Sensitivity Function (CSF) that represents the relationship between perceptible contrasts and spatial frequencies of visual stimuli is central to these models. Cottaris et al [2] proposed to convert RGB images to cone excitation images, taking into account the wavelength-dependent point spread functions due to the eye optics, absorption in lens and macular pigment, and cone mosaic, with all the parameters extracted from physiological measurements. The CS derived from this method are in close agreement with the one measured in the standard experiment. Pattern sensitivity is simulated by a Support Vector Machine (SVM) classifier. Although the introduction of low vision parameters is straightforward in this model, it cannot be directly used for our purpose, as it is restricted to simple pattern stimuli, and hardly adapted to more complex stimuli. Peli [3] set out to define contrast in natural images by taking into account the existence of frequency selective perceptual channels in SVH, and developed a method for simulating perception by a visually impaired subject, based on SVH nonlinearities and experimental CSF measurements. Thomson et al [4] contributed to extend this work, first by establishing a method for parametrization of standard analytical CSF model with classical clinical acuity and contrast sensitivity measurements. They have also proposed to handle color images, by translating them from RGB to CIE xyY color spaces, and then, by using CSF as a linear band pass filter for the two chromatic x and y channels. Al Atabany et al [5] implemented a degenerative retina model with central scotoma, based on mathematical ex-

pressions of connectivity between the different neural layers within the retina. This approach allowed them to simulate foveal center-surround processing and color opponency mechanisms. Consequences of ageing on visual performances are another area where simulation approach is developed [6, 7]. Age dependent parameters such as reduced pupil size, increased scattering in ocular media and diminution of retinal cell density are introduced in standard CSF expressions.

3 The computational low vision model

Our model is intended to simulate foveal vision in photopic conditions, for viewing natural scene images on electronic displays, and therefore is concerned by color perception, light adaptation and masking effects. It must be applicable whatever the display technical characteristics, lighting conditions and distance to the screen.

3.1 Standard vision modeling

Among the numerous models of CSF that have been employed for instance in image quality assessment, we have chosen to build our work on Barten's model [8], as it explicitly decomposes the CSF into successive components corresponding to optical, retinal and neural processing. As it was based on luminance sine wave gratings with limited spatial frequency contents, it has to be completed to take in account wide band color stimuli.

Our model consists in four steps. The first step corresponds to pre retinal processing. RGB image is converted in device-independent and position-independent image in the CIE xyY color space. This image is then filtered by a lowpass Gaussian function modeling the Optical Transfer Function (OTF).

$$OTF(u) = e^{\left(-2.\left(\pi.\sqrt{(\sigma_0^2+(C_{ab}.d).^2)}.u\right)^2\right)} \quad (1)$$

where u is the spatial frequency (expressed in cpd) and d the pupil size, depending on luminance adaptation level. This level is calculated by averaging Y values on the whole image, if the assumption is made that image is seen in a dark room. Otherwise, it can be set to the ambient luminance level. The σ_0 value depends on diffusion in lens and ocular media and on photoreceptor density.

The second step corresponds to retinal processing. Assuming separability between color and pattern sensitivity, separate CSF may be implemented for luminance and chromatic channels. Cone excitation image is obtained by a conversion in LMS color space, based on Smith and Pokorny approximation, and then recoded as a contrast image: for each L, M ou S component, each pixel value is divided by the mean value of its neighborhood, whose size is similar to the one used in lateral inhibition process. Neural processing that occurs in the following layers in the retina is simulated by conversion into the Krauskopf color opponent space [9]. For the achromatic components, we use the highpass function developed by Barten. He considers that lateral inhibition (modeling center surround effect because of connectivity between cones, horizontal

cells and bipolar cells) is applied to visual stimuli summed with photon noise (fluctuation in the number of photons actually initiating cone excitation) and neural noise (intrinsic fluctuations in neural signals):

$$M(u) = \frac{1}{k.\sqrt{\left(\frac{2}{T}.\left(\frac{1}{X_0^2}+\frac{1}{X_{max}^2}+\frac{u}{N_{max}^2}\right)\left(\frac{1}{\eta.p.E}.\left(\frac{\phi_0}{\left(1-e^{(-(u/u_0)^2)}\right)}\right)\right)\right)}} \quad (2)$$

where k is the Signal to Noise Ratio (SNR) allowing detection, T is the integration time of the eye, X_0 is the integration area angular size, N_{max} is the number of cycles over which the eye can integrate, η is the quantum efficiency, p is the photon conversion factor, E is the retinal illuminance, Φ_0 is the spectral density of neural noise, u_0 is the spatial frequency above which lateral inhibition disappears. For the chromatic red-green and blue –yellow components, we use the lowpass sensitivity functions described in [9].

The third step is a rough representation of the first V1 area in the visual cortex, where visual information is known to be processed by separate frequency and orientation selective cells. It is based on the Cortex transform [10]. Contrast image is decomposed into a set of subband images. In each of these image, masking effect is implemented according to [11]: contrast perception is a nonlinear process, with threshold dependent both on the contrast value and on the entropy of its neighborhood.

The last step is the reconstruction of perceived image: in each frequency subband achromatic image, each pixel value is compared to the corresponding threshold, given by CSF. Values below threshold are replaced by the local mean luminance, while values above are not modified. Thresholded achromatic and chromatic subband images are then summed, and the resulting image translated back to RGB space. The sum is restricted to the subbands that can actually be displayed by the screen, depending on its resolution.

3.2 Low vision modeling

As a first example, we choose to simulate low vision observer suffering from Retinitis pigmentosa (RP), an inherited retinal degenerative disease leading to the loss of photoreceptors. The first symptoms of RP are night blindness and light sensitivity, before progressive constriction of peripheral field of view [12]. Patients also report that colors appear to them as dull and washed out. Some of the model parameters have to be modified to match the pathological retina characteristics. The loss of photoreceptors is simulated by applying a factor C_{loss} lower than unity to the LMS cone response values. According to [13], foveal acuity may remained unchanged with as much as a cone loss of about 40%, and 20/50 vision is expected with only 10% of foveal cones. It is likely to assume that, among all the parameters included in the CSF model, the quantum efficiency (η), the standard deviation (σ_0) which relies on cone density and the SNR (k) have to be modified to correspond to a RP observer. Their values were varied to fit CSF from RP patients. Figure 1 shows simulation of perceived images by normal and

low vision observers. The standard observer model is based on parameter values defined in [8], and the impaired ones on values chosen to fit real individual CSF, found in [14].

(a) (b) (c)

Fig. 1. Simulation of images perceived by normal and visually impaired individuals. (a): standard observer ($k = 3$, $\eta = 0.03$, $\sigma_0 = 0.5$ arcmin) ; (b) visual acuity 0.4 ($k = 45$, $\eta = 0.01$, $\sigma_0 = 4$arcmin, $C_{loss} = 0.75$); (c): visual acuity 0.2 ($k = 75$, $\eta = 0.01$, $\sigma_0 = 6$ arcmin, $C_{loss} = 0.5$)

4 Contrast enhancement algorithm comparison

The model relevance is demonstrated by its application on images processed by three contrast enhancement algorithms. The simulated perceived images appear to be different, and suggest modifications to improve their efficiency. An attempt to quantify these differences is made, relying on blur measurement and color saturation.

4.1 Contrast enhancement algorithm

The first algorithm is the classical unsharp masking, with a 5x5 pixels Laplacian filtered image added to the initial image [15]. This algorithm is applied in RGB space. The second one is a cartoonization algorithm, as described in [5], with original RGB image Gaussian blurring, conversion to YCbCr color space, anisotropic difference filtering applied on the luminance channel, and color quantization in sixteen levels. The third algorithm is a customization of the second one, with addition of supplementary steps of luminance channel unsharpening and increase of color saturation: chrominance values are multiplied by a constant (equal to 4 in the following examples).

4.2 Blur improvement index

The measurement of image blurriness appears to be relevant as these algorithms are intended to improve the perception of images blurred by low acuity. The edge sharpness is strongly correlated with the amount of the existing blur in any image. A blur improvement index is computed according to the method described in [16]: for every pixel in both the reference image and the blurred image, the difference is computed between the center pixel and its height neighbor pixels, and the maximum value is calculated. Then, the average Z1 and Z2 of this maximum is calculated on the two whole images.

The blur improvement index BI is calculated by the difference between Z1 and Z2. The most blurred is the processed image relative to the original, the most BI tends to 0.

4.3 Color saturation assessment

The cone losses in degenerative retina involve modifications in color vision. At the middle stage of the disease, environment is perceived as fade and dull. So the color saturation in processed images is a good indicator of visual perceptibility improvement. Saturation amplitude is calculated as the square rooted sum of the two squared chrominance components. Saturation index is calculated as the ratio between the saturation maximum of processed image to the maximum saturation of original image.

5 Results

The previously described algorithms were applied to 16 images extracted from the Kodak database (www.cs.albany.edu/~xypan/research/snr/Kodak.html), which are then processed by the low vision observer with visual acuity: 0.4. (figure 2).

Blur improvement index and color saturation index calculated for each image compared to the initial image are resumed in table 1.

Table 1. Comparison

	Blur improvement index	Saturation index
Perceived original image	0.23	0.20
Perceived processed image (unsharp masking)	0.37	0.22
Perceived processed image (cartoon)	0.21	0.3
Perceived processed image (customized cartoon)	0.25	0.40

The perceived original image is significantly degraded, in terms of blur and color attenuation. Unsharp masking appears as the most efficient in blur reduction, but has minor effect on color saturation. This may explain why it was rejected by subjects in [15]. Cartoonization algorithm does not significantly improve both criteria. Increase of color saturation is only performed by the supplementary step added to the customized cartoon algorithm. It appears that using the low vision observer model might be helpful when investigating for enhancement algorithms with better efficiency for the visually impaired.

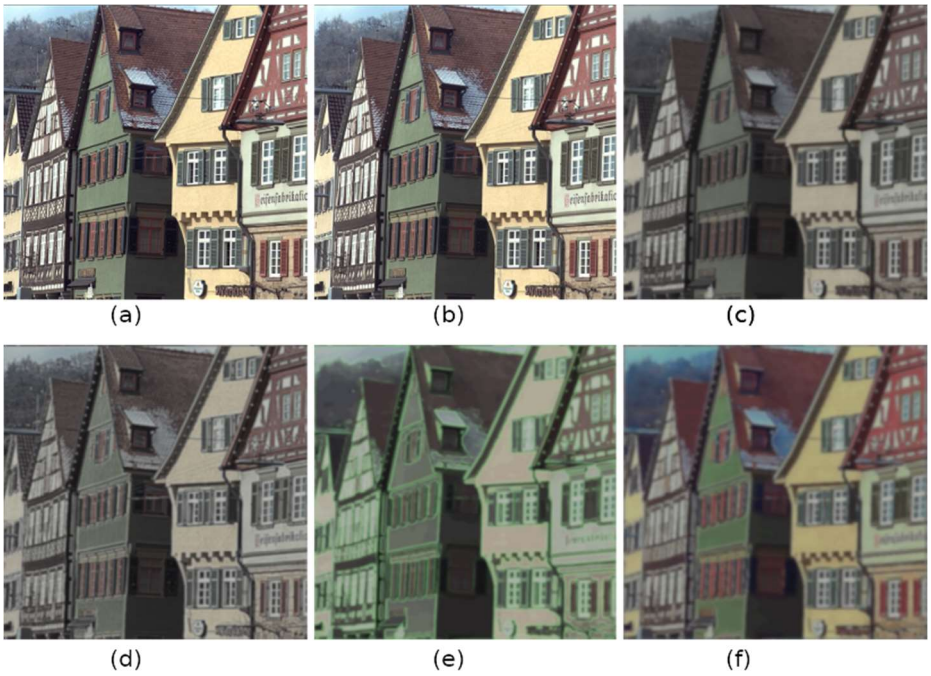

Fig. 2. Simulation of perceived images by a standard observer and a low vision observer (visual acuity: 0.4). (a): original image, (b): original image for standard observer, (c) original image for low vision observer, (d) processed image for low vision observer (unsharp filter), (e) processed image for low vision observer (cartoon filter),(f): processed image for low vision observer (customized cartoon filter)

6 Conclusion

This paper presents the first results related to a computational model of low vision observer. Its application gives cues for implementation of more efficient enhancement algorithms. Future works include further investigations on objective criteria for the measure of perceptibility increase, and experimental validation by comparison with human ranking on processed images.

References

1. Moshtael, H., Aslam, T., Underwood, I., & Dhillon, B. High tech aids low vision: a review of image processing for the visually impaired. Translational vision science & technology, *4*(4), 6-6, (2015)

2. Cottaris, N. P., Jiang, H., Ding, X., Wandell, B. A., & Brainard, D. H. A computational-observer model of spatial contrast sensitivity: Effects of wave-front-based optics, cone-mosaic structure, and inference engine. Journal of vision, *19*(4), 8-8. (2019)
3. Peli, E. Simulating normal and low vision. Vision Models for Target Detection and Recognition,. E. Peli, ed. World Scientific (1995)
4. Thompson, W. B., Legge, G. E., Kersten, D. J., Shakespeare, R. A., & Lei, Q. Simulating visibility under reduced acuity and contrast sensitivity. JOSA A, *34*(4), 583-593 (2017)
5. Al-Atabany, W. I., Memon, M. A., Downes, S. M., & Degenaar, P. A. Designing and testing scene enhancement algorithms for patients with retina degenerative disorders. Biomedical engineering online, 9(1), 27. (2010).
6. Joulan, K., Brémond, R., & Hautière, N. Towards an analytical age-dependent model of contrast sensitivity functions for an ageing society. The Scientific World Journal, (2015)
7. Mantiuk, R. K., & Ramponi, G. Age-dependent prediction of visible differences in displayed images. Journal of the Society for Information Display, 26(1), 4-13 (2018).
8. Barten, P. G. (Contrast sensitivity of the human eye and its effects on image quality. SPIE press.(1999)
9. Le Callet, P., & Barba, D.Robust approach for color image quality assessment. In Visual Communications and Image Processing 2003 (Vol. 5150, pp. 1573-1581). International Society for Optics and Photonics. (2003)
10. Watson, A. The cortex transform- Rapid computation of simulated neural images. Computer vision, graphics, and image processing, 39(3), 311-327 (1987)
11. Ninassi, A., Le Meur, O., Le Callet, P., & Barba, D. On the performance of human visual system based image quality assessment metric using wavelet domain. Proc. SPIE Human Vision and Electronic Imaging XIII, vol. 6806 (2008)
12. Hartong, D. T., Berson, E. L., & Dryja, T. P. Retinitis pigmentosa. The Lancet, 368(9549), 1795-1809 (2006)
13. Bensinger, E., Rinella, N., Saud, A., Loumou, P., Ratnam, K., Griffin, S. & Duncan, J. L. Loss of Foveal Cone Structure Precedes Loss of Visual Acuity in Patients With Rod-Cone Degeneration. Investigative ophthalmology & visual science, 60(8), 3187-3196 (2019)
14. Hyvârinen, L., Rovamo J., Laurinen, P., & Peltomaa, A. Contrast sensitivity function in evaluation of visual impairment due to retinitis pigmentosa. Acta ophthalmologica, 59(5), 763-773(1981)
15. Leat, S. J., Omoruyi, G., Kennedy, A., & Jernigan, E. Generic and customized digital image enhancement filters for the visually impaired. Vision research, 45(15), 1991-2007(2005)
16. Elsayed, M., Sammani, F., Hamdi, A., Albaser, A., & Babalghoom, H. A new method for full reference image blur measure. International Journal of Simulation: Systems, Science Technology, vol. 19, pp. 4, 05 (2018)